

Elastic constants of $\text{Ti}_{50}\text{Ni}_{30}\text{Cu}_{20}$ alloy prior to martensitic transformation

By X. REN[†], K. TANIWAKI[†], K. OTSUKA[†], T. SUZUKI[‡], K. TANAKA[§],
YU. I. CHUMLYAKOV[¶] and T. UEKI^{||}

[†] Institute of Materials Science, University of Tsukuba, Tsukuba,
Ibaraki 305-8573, Japan

[‡] Tsukuba Institute of Science and Technology, Tsuchiura, Ibaraki 300-0811,
Japan

[§] Department of Materials Science, Kyoto University, Kyoto 606-8501, Japan

[¶] Siberian Physical Technical Institute, Tomsk 634050, Russia

^{||} Yokohama R&D Laboratory, The Furukawa Electric Co. Ltd., Nishi-Ku,
Yukohama 220-0073, Japan

[Received 27 January 1998; revised version accepted 27 February 1998]

ABSTRACT

Elastic constants of $\text{Ti}_{50}\text{Ni}_{30}\text{Cu}_{20}$ alloy prior to the martensitic transformation $\text{B2} \rightarrow \text{B19}$ was measured for the first time by using the rectangular parallelepiped resonance method. The softening in both shear modulus c and c_{44} was found with approaching transformation temperature. As a result of soft c_{44} , the anisotropy factor shows a low value of 2.8 in the vicinity of the transformation temperature. c_{11} , c_{12} , and bulk modulus were found to show little temperature dependence in the vicinity of the transformation temperature. Compared with the binary $\text{Ti}_{50}\text{Ni}_{50}$ alloy, $\text{Ti}_{50}\text{Ni}_{30}\text{Cu}_{20}$ alloy exhibits a 40% higher and increasing anisotropy with approaching transformation temperature. Based on the experimental results, we explained why $\text{Ti}_{50}\text{Ni}_{30}\text{Cu}_{20}$ transforms into B19 martensite, while $\text{Ti}_{50}\text{Ni}_{50}$ transforms into a strange monoclinic $\text{B19}'$ martensite.

§1. INTRODUCTION

Despite the fact that Ti–Ni is the most important shape memory alloy for various technological applications (for example, Otsuka and Shimizu (1986)), its martensitic transformation (MT) mechanism, which governs its properties, has remained poorly understood for many years compared with other shape memory alloys. The central problem is how to explain the abnormal structure of TiNi martensite $\text{B19}'$.

In contrast to other martensites of β (B2) phase alloys which are invariably formed by different ways of basal plane stacking (see Nishiyama (1978) for a review), $\text{B19}'$ martensite exhibits a large and strange non-basal distortion ($\{001\}\langle 110 \rangle_{\text{B2}}$ shear) to the well-known basal plane structure B19 (Heheman and Sandrock 1971, Kudoh *et al.* 1985). This non-basal shear gives a monoclinic distortion to B19 structure and lowers the orthorhombic symmetry of B19 to monoclinic, thus the distorted martensite is named as $\text{B19}'$. The reason for such a non-basal distortion is unclear. On the other hand, the addition of 20 at.% Cu into $\text{Ti}_{50}\text{Ni}_{50}$ alloy changes the transformation product into common B19 martensite for $\text{Ti}_{50}\text{Ni}_{30}\text{Cu}_{20}$ alloy (Nam *et al.* 1990b), although the parent phase for both alloys has the same B2 (CsCl) structure. Accompanying such a change of transformation product, the

transformation hysteresis shows a dramatic change, being about 4 K for the B2-B19 transformation (Nam *et al.* 1990b), in contrast to about 30 K for B2-B19' transformation. Furthermore, an intermediate alloy $\text{Ti}_{50}\text{Ni}_{40}\text{Cu}_{10}$ shows an intermediate transformation behaviour: it transforms into B19 martensite first and then the B19 transforms into B19' at a lower temperature (Nam *et al.* 1990a). We expect that the origin of the non-basal distortion in TiNi, which is responsible for the monoclinicity in B19' martensite, can be found if we can understand why such a distortion disappears in the $\text{Ti}_{50}\text{Ni}_{30}\text{Cu}_{20}$ alloy.

Unlike diffusional transformations which are mainly controlled by configurational energies, a martensitic transformation involves only cooperative atomic displacement or lattice distortions without atom exchange or diffusion, and thus lattice dynamics play a key role in MT, as manifested by recent neutron scattering experiments (Shapiro *et al.* 1989, Manósa *et al.* 1993, Ohba *et al.* 1994), elastic constant measurements (Mercier *et al.* 1980, Khachin *et al.* 1987, Brill *et al.* 1991), and theoretical studies (Barsch and Krumhansl 1984, Krumhansl and Gooding 1989). Therefore, the influence of alloying element and lattice defect on MT should stem from their influence on lattice dynamics. For example, a 2.5 at.% decrease in Cd content for $\text{Au}_{50}\text{Cd}_{50}$ alloy leads to a 30% decrease in shear modulus c' ($= (c_{11} - c_{12})/2$) (Zirinski 1956) and an appreciable modification to phonon dispersion relation (see relevant data of Ohba *et al.* (1994, 1998)), and consequently results in a completely different martensite structure with a ~ 40 K increase in transformation temperature (Sakamoto *et al.* 1990). Quenching which creates point defects was also found to have a similar effect which changes elastic constants as much as 30% and may lead to a different martensite (Zirinski 1956). These facts are in sharp contrast to the insensitivity of elastic constants to alloying and defects for non-transforming alloys. In table 1 we compiled some available experimental data (Zirinski 1956, Gray 1972, Verlinden and Delaey 1986) of the composition dependence of elastic constants for non-transforming and transforming alloys. It is notable that transforming alloys generally have a much stronger composition dependence of elastic constants, especially for c' , compared with non-transforming alloys. This strongly suggests that MT is controlled by lattice dynamics, thus the effect of alloying and defects is due to their influence on lattice dynamics.

Elastic constant measurement is an effective and easy way to obtain information about the lattice dynamics, especially on the harmonic part of the lattice energy. However, there have been only a few elastic constant measurements on TiNi to date (Mercier *et al.* 1980, Khachin *et al.* 1987, Brill *et al.* 1991), and no elastic constants are known for the ternary alloy TiNiCu. This is mainly due to the difficulty in growing single crystals of these alloys.

There have been numerous experimental data showing that prior to MT a (partial) softening in c' occurs, which signals a reduced resistance to $\{110\}\langle 110 \rangle_{\text{B2}}$ basal shear that is responsible for forming basal-plane based martensites, such as B19(2H), 3R, 6R, 7R, 9R, and 18R. However, as mentioned above, this shear alone is insufficient to create the monoclinic B19' structure of TiNi, which requires an additional $\{001\}\langle 110 \rangle_{\text{B2}}$ non-basal shear to distort the basal structure B19. The shear modulus corresponding to this additional shear can be simply proved to be c_{44} for cubic crystals (which is also $\{001\}\langle 100 \rangle_{\text{B2}}$ shear modulus by definition). Therefore, we can anticipate that c_{44} is important to understand MT in TiNi and its ternary alloys.

The purpose of the present paper is to measure the elastic constants of $\text{Ti}_{50}\text{Ni}_{30}\text{Cu}_{20}$ alloy by rectangular parallelepiped resonance (RPR) method, and to

Table 1. Sensitivity of elastic constants to composition variation for non-transforming and transforming alloys.^{a,b}

Category	Alloy (composition: x at.%)	$\left \frac{dc'}{c' dx} \right $	$\left \frac{dc_{44}}{c_{44} dx} \right $	$\left \frac{dc_{11}}{c_{11} dx} \right $	$\left \frac{dc_{12}}{c_{12} dx} \right $	Reference
Non-transforming alloy	Ag-0-75% Au	0.2-0.4	0.2-0.4	0.3-0.5	0.3-0.6	Gray (1972)
	Cu-0-4.17% Si	~1.8	~0.2	~0.1	~0.6	Gray (1972)
	(α -)Ag-0-2.4% Zn	~1.8	~0.3	~0.5	~0.8	Gray (1972)
	(α -)Cu-0-9.98% Al	~1.1	~0.1	~0.5	~0.3	Gray (1972)
(α -)Cu-0-22.7% Zn	~1.0	~0.3	~0.7	~0.6	Gray (1972)	
Transforming alloy	(β -)Cu-44.9-50% Zn	4-20	~2.9	~2.3	~2.0	Verlinden and Delaey (1986)
	(β -)Au-47.5-50% Cd	~10	~1.1	~2.0	~3.0	Zirinski (1956)
	(b-)Ag-45-50% Zn	1.7-18	—	—	—	Verlinden and Delaey (1986)

^a $|dc/c dx|$ represents the change in percentage of a certain elastic constant c by 1 at.% composition x change, and is a measure of the sensitivity of elastic constants to composition change. Because of the nonlinear composition dependence of elastic constants, $|dc/c dx|$ is dependent on composition, thus an approximate value or a range of the value is given.

^b In certain composition ranges of some transforming alloys (e.g. Cu-Zn), the transformation temperature is lowered below 0 K so the alloys appear to be non-transforming. However, they are inherently transforming alloys because the transformation may occur if additional energy is provided, such as stress or hydrostatic pressure.

compare them with the available data of $Ti_{50}Ni_{50}$ in order to understand how martensite structure and transformation hysteresis is changed by Cu addition. This work will be complemented by an ongoing neutron inelastic study of the same alloy (Taniwaki 1998), and other elastic constant measurements on the intermediate alloy $Ti_{50}Ni_{40}Cu_{10}$ (Miura 1998).

§2. EXPERIMENTAL

2.1. Alloy preparation and heat treatment

$Ti_{50}Ni_{30}Cu_{20}$ single crystal was grown by using a modified Bridgman method in a graphite crucible. After spark cutting into proper sizes, the crystal was solution treated at 1173 K for 1 h in Ar atmosphere, and then quenched into ice water. After the heat-treatment, surface layer was removed by sand-paper polishing and chemical etching. By chemical analysis the true composition of the alloy was found to be $Ti_{49.54}Ni_{30.24}Cu_{20.22}$, being essentially the same as the nominal composition. The nominal transformation temperatures were determined by electrical resistivity measurement in figure 1 to be: $M_s = 318$ K, $M_f = 309$ K, $A_s = 314$ K, $A_f = 321$ K. Here M_s and M_f are martensite start and finish temperatures, while A_s and A_f are reverse transformation start and finish temperatures, respectively. It is interesting to

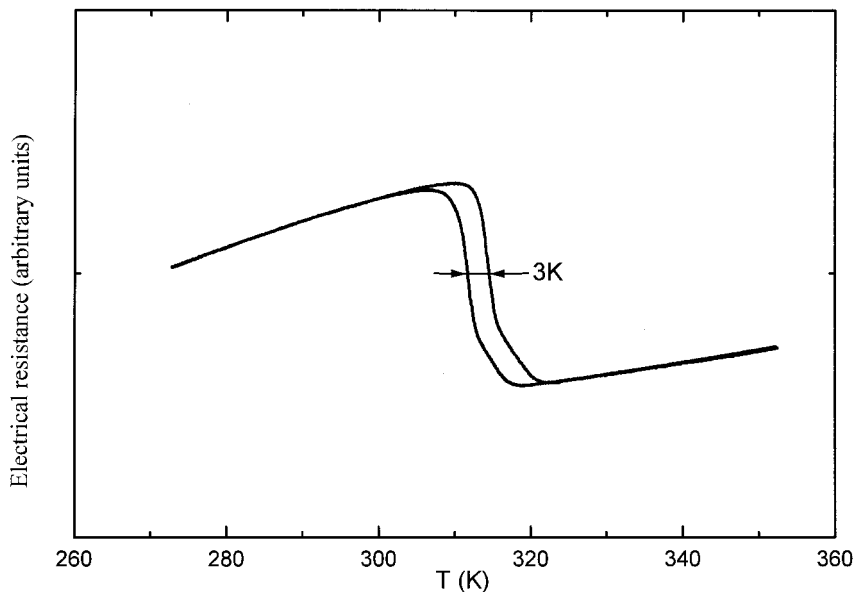


Figure 1. Transformation temperature and hysteresis of martensitic transformation in $\text{Ti}_{50}\text{Ni}_{30}\text{Cu}_{20}$ alloy single crystal determined by electrical resistance measurement.

note that this alloy shows a remarkably small transformation hysteresis (~ 3 K), in contrast to ~ 30 K for Ti–Ni binary alloys.

2.2. Specimen size, density, and orientation accuracy

A sample for elastic constant measurements was cut into a rectangular parallelepiped shape with a size of $4.257 \text{ mm} \times 2.680 \text{ mm} \times 2.290 \text{ mm}$. Its surface normals are in three $\langle 100 \rangle$ directions with an uncertainty less than 1.5° . The density of the alloy in the parent state (around 373 K) was measured to be 6.28 g cm^{-3} , and no correction for thermal expansion was applied due to the large change in elastic constants. With the RPR method, this sample alone was enough to obtain all the elastic constants of $\text{Ti}_{50}\text{Ni}_{30}\text{Cu}_{20}$ alloy prior to MT. Measurement was carried out in the temperature range 323 K – 583 K for the parent phase.

2.3. Elastic constants measured by rectangular parallelepiped resonance

The principle of the RPR method in measuring elastic constants of single crystals was established by Demarest (1971) and further developed by Ohno (1976). The RPR method has found increasing and successful applications in recent years (Migliori *et al.* 1993, Inohara and Suzuki 1993, Tanaka *et al.* 1996a, b). Here we give only a brief description of the basic principle and experimental setting. Interested readers may refer to Tanaka *et al.* (1996b) for more details.

When a sample is allowed to vibrate freely, it exhibits a spectrum of resonance frequencies which corresponds to all the deformation modes and depends on all the elastic constants. If the resonance spectrum is experimentally measured, all the elastic constants can be obtained by best-fitting the theoretical spectrum calculated from Demarest-Ohno theory to the experimental one. Experimentally, the resonance spectrum is measured by lightly holding a rectangular parallelepiped sample body-diagonally between a driving transducer and a receiving transducer such that the

sample can vibrate nearly freely. (In the present experiment we used PZT transducers). By sweeping the frequency of a sinusoidal electrical signal input into the driving transducer, the sample was forced to vibrate with the sweeping frequencies. When the sweeping frequency comes into coincidence with a resonance frequency of the sample, a large vibration occurs and this signal is detected by the receiving transducer and converted into electrical signal and then recorded by a computer. With a complete sweeping from low to high frequencies, a spectrum of resonance frequencies is obtained, and elastic constants can then be calculated from the spectrum.

There are two advantages of the RPR method over the conventional pulse-echo method. Firstly, it allows one to use very small single crystals (may be as small as 2 mm in edge length). This is important because it is not easy to grow large single crystals for most materials, especially for Ti-Ni based alloys. Secondly, this method can be easily extended to measure elastic constants at high temperature if buffer rods are used to separate the high temperature specimen and the transducers. This is indispensable for pre-transformation study because the change of elastic constant over a wide temperature range is more important than the absolute value.

An example of the comparison between the calculated spectrum obtained from the optimized elastic constants and experimental spectrum for $Ti_{50}Ni_{30}Cu_{20}$ alloy is shown in figure 2. Over 60 resonance frequencies are used during the optimization. Instead of using c_{11} , c_{12} and c_{44} during the optimization, we used $\nu (= c_{12}/(c_{11} + c_{12}))$, $A (= c_{44}/c')$ and c_{44} to make the calculation easier. With the optimized elastic constants we found the average difference between calculated and experimental frequencies for all temperatures is less than 0.55%. Some missing resonance frequencies arises from the fact that not all resonance vibrations are excited to a detectable magnitude by the driving transducer. During the best-fitting, we plotted the temperature dependence of frequencies of all deformation modes to eliminate incorrect

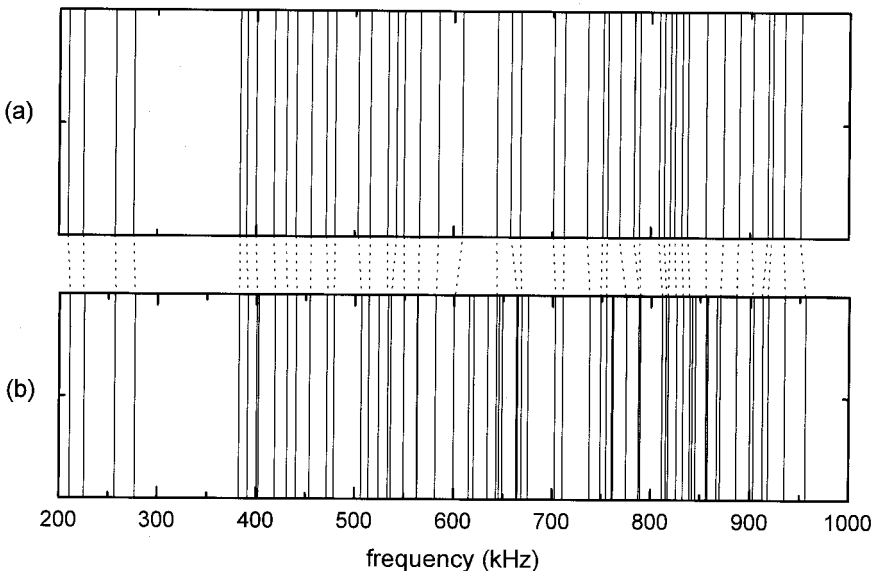


Figure 2. Comparison between (a) experimental resonance spectrum and (b) calculated one from the optimized elastic constants at 343 K.

mode-identification, because in the case of an incorrect mode identification the corresponding mode frequencies would show an unnatural temperature dependence. Considering the error in orienting the sample surface and the scattering of the data, we estimate that in the present measurement the maximum errors are 1% for c' , 2% for c_{44} , and 5% for c_{11} and c_{12} , respectively. It should be noted that the uncertainty of RPR method is smaller for c' and c_{44} than for c_{11} and c_{12} . This is due to the fact that c' and c_{44} are mainly related to low frequency resonance which can be determined more accurately (Inohara and Suzuki 1993) This is also an advantage for MT study because c' is of the closest relevance.

§3. EXPERIMENTAL RESULTS

For cubic crystals there exist only three independent elastic moduli, usually taken as c_{11} , c_{12} , and c_{44} , and the rest can be calculated from these three. However, for martensitic transformation $c' = (c_{11} - c_{12})/2$ is important because it is related to $\{110\}\langle\bar{1}10\rangle_{B2}$ basal shear mode. Anisotropy factor $A = c_{44}/c'$ is also known to be important for martensitic transformation. Thus in the following we give all elastic constants, including c_{11} , c_{12} , c_{44} , c' , and bulk modulus $B = (c_{11} + 2c_{12})/3$, as well as anisotropy factor A . We also include the corresponding data of equi-atomic $\text{Ti}_{50}\text{Ni}_{50}$ (after Mercier *et al.* (1980), the nominal composition of their alloy is $\text{Ti}_{50.1}\text{Ni}_{49.9}$) for comparison.

The measured elastic constants c' , c_{44} , anisotropy factor A , c_{11} , c_{12} , and B as a function of temperature in the parent B2 phase above M_s temperature are tabulated in table 2, and these data are shown in figures 3(a)–(d).

Table 2. Elastic constant data of $\text{Ti}_{50}\text{Ni}_{30}\text{Cu}_{20}$ alloy in the parent phase prior to martensitic transformation. Uncertainty of the data: T : < 0.5 K, c : 1%, c_{44} : 2%, c_{11} and c_{12} : 5%.

T (K)	$c' = (c_{11} - c_{12})/2$ (GPa)	c_{44} (GPa)	$A = c_{44}/c'$	c_{11} (GPa)	c_{12} (GPa)	$B = (c_{11} + 2c_{12})/3$ (GPa)
323	12.9	36.4	2.813	209	183	192
328	12.2	36.6	2.770	211	184	193
333	13.3	37.0	2.779	206	179	188
338	13.5	37.3	2.756	208	181	190
343	13.6	37.5	2.749	214	187	196
348	13.7	37.8	2.752	214	186	195
353	13.9	38.1	2.748	205	178	187
358	14.0	38.3	2.731	207	178	188
363	14.1	38.6	2.731	207	179	188
368	14.3	38.8	2.722	231	182	192
373	14.4	38.9	2.707	211	183	192
383	14.6	39.4	2.700	213	184	194
403	15.2	39.9	2.629	208	177	187
423	15.7	40.2	2.568	204	173	183
443	16.0	40.8	2.545	210	178	189
463	16.3	41.5	2.543	208	176	186
483	16.6	41.9	2.524	204	171	182
503	17.0	41.6	2.453	203	169	181
523	17.1	42.3	2.481	205	171	183
543	17.4	42.4	2.444	202	167	179
563	17.6	42.6	2.421	203	168	180

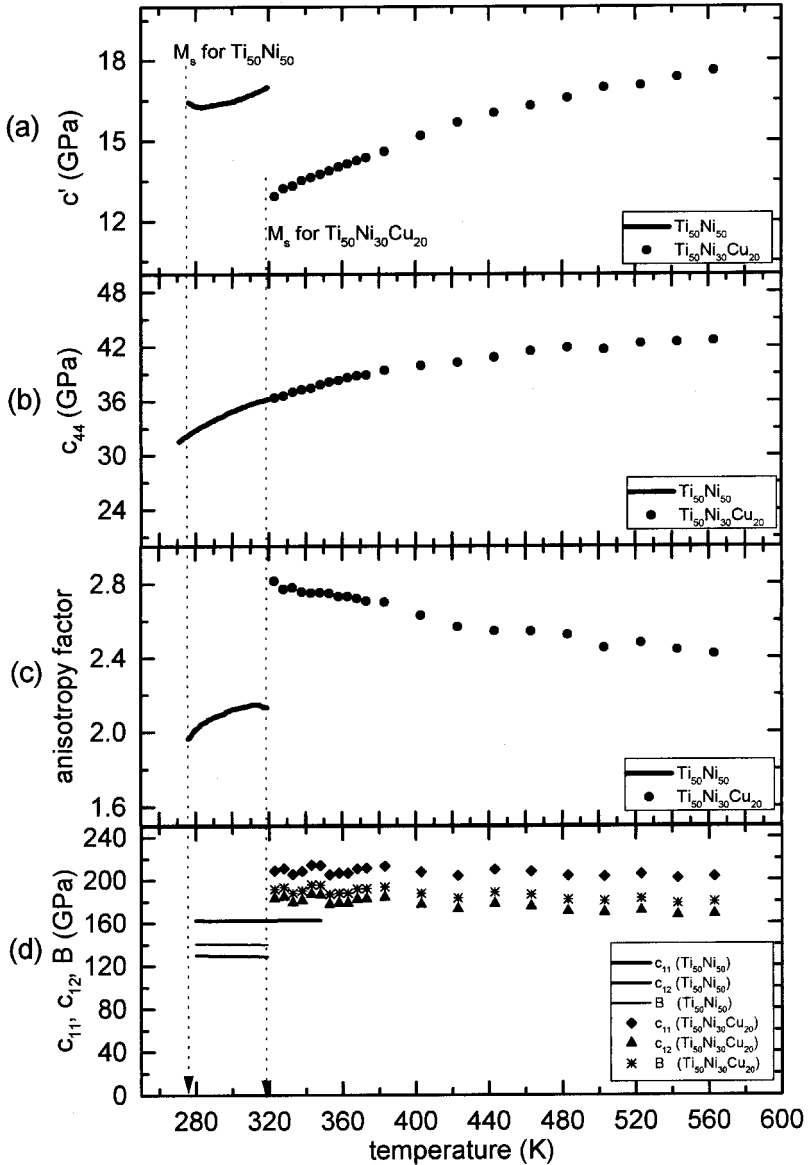


Figure 3. Temperature dependence of (a) c' , (b) c_{44} , (c) anisotropy factor and (d) c_{11} , c_{12} , B for $Ti_{50}Ni_{30}Cu_{20}$ and $Ti_{50}Ni_{50}$ alloys.

3.1. c' , c_{44} and anisotropy factor

From figure 3(a), we can see that c' shows a partial softening prior to MT. This behaviour is similar to all other alloys showing MT, and is an indication that the parent lattice is becoming unstable to a $\{110\}\langle 110 \rangle$ shear which deforms the parent B2 structure into layered martensite structures with $\{110\}_{B2}$ stacking. Compared with $Ti_{50}Ni_{50}$ binary alloy, $Ti_{50}Ni_{30}Cu_{20}$ alloy shows a 30% lower c' in the vicinity of the M_s temperature. This explains the higher transformation temperature of the ternary alloy, because a lower c' indicates a smaller resistance to the shear transformation.

Figure 3(b) shows a notable result that c_{44} exhibits a softening prior to MT. This behaviour is similar to that of binary $\text{Ti}_{50}\text{Ni}_{50}$. An ongoing experiment (Miura 1998) indicates that a different ternary alloy $\text{Ti}_{50}\text{Ni}_{40}\text{Cu}_{10}$ also exhibits a softening in c_{44} . Therefore, the softening of c_{44} may be common for all the TiNi binary and ternary alloys. Because no softening in c_{44} was found in other alloys with basal stacking martensite structure, it is natural to consider c_{44} to play an important role in creating the strange $\text{B}19'$ martensite structure. Obviously, the softening in c_{44} alone is not sufficient to create $\text{B}19'$ martensite, because $\text{Ti}_{50}\text{Ni}_{30}\text{Cu}_{20}$ alloy shows a very similar softening in c_{44} , but it transforms into common B19 martensite. A detailed discussion will be given later.

Another notable result is the anisotropy factor A and its temperature dependence, as shown in figure 3(c). Compared with the high anisotropic factors (10–20) of β phase alloys, both $\text{Ti}_{50}\text{Ni}_{30}\text{Cu}_{20}$ alloy and $\text{Ti}_{50}\text{Ni}_{50}$ alloy show remarkably low values (2.8 and 2.0 at MT temperature) of elastic anisotropy. Since anisotropy factor is the ratio of c_{44} to c' , a low value of anisotropy indicates that resistance to c_{44} shear and to c' shear is similar, in other words, c_{44} shear and c' shear become more correlated. On the other hand, there are two important differences between $\text{Ti}_{50}\text{Ni}_{30}\text{Cu}_{20}$ and $\text{Ti}_{50}\text{Ni}_{50}$ alloy. Firstly, $\text{Ti}_{50}\text{Ni}_{50}$ alloy has a 40% lower anisotropy than that of $\text{Ti}_{50}\text{Ni}_{30}\text{Cu}_{20}$ in the vicinity of M_s . Secondly, $\text{Ti}_{50}\text{Ni}_{50}$ exhibits a decreasing anisotropy with approaching MT while $\text{Ti}_{50}\text{Ni}_{30}\text{Cu}_{20}$ shows an opposite behaviour. The decreasing anisotropy for $\text{Ti}_{50}\text{Ni}_{50}$ indicates an increasing correlation between c_{44} shear and c' shear towards MT. As will be discussed later, this correlation is crucial to understand why $\text{Ti}_{50}\text{Ni}_{50}$ transforms into $\text{B}19'$ martensite, while $\text{Ti}_{50}\text{Ni}_{30}\text{Cu}_{20}$ transforms into B19 martensite.

3.2. c_{11} , c_{12} and bulk modulus

Elastic constants c_{11} , c_{12} and bulk modulus B for $\text{Ti}_{50}\text{Ni}_{30}\text{Cu}_{20}$ alloy are shown in figure 3(d), together with those of $\text{Ti}_{50}\text{Ni}_{50}$. It is found that $\text{Ti}_{50}\text{Ni}_{30}\text{Cu}_{20}$ alloy has $\sim 20\%$ higher c_{11} , c_{12} and B than those of $\text{Ti}_{50}\text{Ni}_{50}$. In the vicinity of transformation temperature (~ 60 K above M_s), these elastic constants versus temperature curves appear to become flat (within experimental uncertainty), similar to the behaviour of $\text{Ti}_{50}\text{Ni}_{50}$. The flat curves for both $\text{Ti}_{50}\text{Ni}_{30}\text{Cu}_{20}$ and $\text{Ti}_{50}\text{Ni}_{50}$ indicate a weak softening which just balances the normal effect (increases elastic constants with lowering temperature). Since this softening behaviour was also found in another ternary alloy $\text{Ti}_{50}\text{Ni}_{40}\text{Cu}_{10}$ (Miura 1998), it seems to be a common feature of Ti–Ni based alloys. Under suitable thermal treatment or deformation, TiNi binary and ternary alloys are known to form a special martensite called R phase, which was recently identified to possess the same trigonal structure as ζ martensite of Au–Cd alloy (Hara *et al.* 1997). It is interesting to note that Au–Cd alloy also shows a softening in c_{11} and c_{12} (Zirinski 1956), similar to that of TiNi based alloys. Therefore, it seems that the softening in c_{11} and c_{12} (or the related bulk modulus B) may be related to the formation of the trigonal martensite. However, a clear relation has not been established yet.

§4. DISCUSSION

It is not surprising that a softening of the shear modulus c' occurs in $\text{Ti}_{50}\text{Ni}_{30}\text{Cu}_{20}$ prior to MT as shown in figure 3(a), because similar behaviour has been observed for all β phase alloys. The softening in c' signals the decrease in the resistance to $\{110\}\langle 110 \rangle_{\text{B}2}$ basal shear, which brings the closed packed planes $\{110\}_{\text{B}2}$

of the B2 parent phase into martensite basal planes. It has been known that B19(2H), 3R, 6R, 7R, 9R, and 18R martensites are formed by different stacking of the basal planes (Nishiyama 1978).

One of the most notable feature of elastic constants of Ti–Ni and Ti–Ni–Cu alloys is that c_{44} shows a softening prior to MT, as concluded from $Ti_{50}Ni_{50}$ binary alloy (Mercier *et al.* 1980), $Ti_{50}Ni_{30}Cu_{20}$ (present study) and $Ti_{50}Ni_{40}Cu_{10}$ (Miura 1998). This feature just coincides with a long-standing unknown fact that some of the binary and ternary Ti–Ni alloys transform into a B19' martensite, which exhibits an unexpected non-basal plane (or non-close-packed plane) shear to the basal plane stacking structure (B19). Such a non-basal shear is a challenge to the well-accepted basal shear picture of martensitic transformation that relies on the softening of the basal shear modulus c' and the related phonon. It is reasonable to consider that the B19' has some relation with the softening in c_{44} .

Since a detailed analysis and modelling of the important role of c_{44} in determining the non-basal shear in B19' will appear elsewhere (Ren and Otsuka 1998), here we only briefly discuss the essential points. Martensitic transformation is a strain transformation which in principle allows all different strain components to be incorporated into the transformation. If one strain mode (usually c' shear) becomes very soft, it dominates the MT and leads to a martensite structure characterized by this strain mode. If another strain mode (say c_{44} shear) becomes soft enough and comparable with c' mode, a correlation of this mode with c' mode is produced, then the resultant martensite structure is characterized by both c' shear and the c_{44} shear, such a structure is what we called B19' martensite. It is easy to prove that the non-basal c_{44} shear is responsible for the non-basal $\{001\}\langle 110 \rangle_{B2}$ shear for B19' martensite, because c_{44} represents the resistance to $\{001\}\langle 110 \rangle_{B2}$ shear. (It is also the $\{001\}\langle 100 \rangle_{B2}$ shear modulus.) It is natural that the coupling between c' and c_{44} determines the occurrence of non-basal shear or the B19' structure. Since the coupling is dependent on the difference between c' and c_{44} or anisotropy factor $A = c_{44}/c'$, a low anisotropy factor is a necessary condition to form the B19' structure. Binary $Ti_{50}Ni_{50}$ has a low and decreasing A (~ 2.0), thus it transforms into B19' martensite. With the addition of 20% Cu to substitute Ni, the resultant $Ti_{50}Ni_{30}Cu_{20}$ alloy has a 40% increase in anisotropy, thus the coupling between c' shear and c_{44} shear becomes much weakened and this leads to the formation of B19 martensite without non-basal c_{44} shear. The weakening of the coupling in $Ti_{50}Ni_{30}Cu_{20}$ can also be understood from the increasing anisotropy with decreasing temperature. Therefore, we can clearly see that the effect of alloying on martensite structure is to change the lattice dynamics through changing elastic constants (and phonon energies in general).

Based on the above reasoning we can make a prediction about the stress-induced MT behaviour of $Ti_{50}Ni_{30}Cu_{20}$ alloy. We predict that B19' martensite can be formed in $Ti_{50}Ni_{30}Cu_{20}$ alloy if we exert $\{001\}\langle 110 \rangle_{B2}$ shear to the parent phase, although only B2–B19 transformation occurs during cooling. This is based on the observed softening in c_{44} , which indicates a potential ability to transform into B19' martensite. If we assist the transformation by adding $\{001\}\langle 110 \rangle_{B2}$ shear, B19' may be formed after a prior transformation to B19, then the stress-strain curve will show two stages, one corresponds to B2–B19, and another corresponds to B19–B19'. This prediction awaits experimental verification, and is also a test to the above explanation.

Based on the present study, we are also able to understand why $Ti_{50}Ni_{30}Cu_{20}$ exhibits smaller transformation hysteresis compared with that of $Ti_{50}Ni_{50}$. As is well

known, transformation hysteresis is due to the existence of nucleation barrier in first order transformation (Rao and Rao 1978). For martensitic transformations the barrier is mainly due to strain energy, which is closely related to the magnitude of lattice deformation for the transformation and the shear modulus of the parent phase (because martensitic transformation is of shear character). Because $\text{Ti}_{50}\text{Ni}_{30}\text{Cu}_{20}$ has a lower c' compared with that of $\text{Ti}_{50}\text{Ni}_{50}$, and it has been known that the former has smaller lattice deformation during transformation than the latter (Chumlyakov *et al.* 1997), thus it is a natural result that $\text{Ti}_{50}\text{Ni}_{30}\text{Cu}_{20}$ shows much smaller hysteresis than $\text{Ti}_{50}\text{Ni}_{50}$.

§5. CONCLUSIONS

In this study, we measured the elastic constants of ternary $\text{Ti}_{50}\text{Ni}_{30}\text{Cu}_{20}$ alloy for the first time. We found that c_{44} shows some softening along with a softening in c' , while c_{11} and c_{12} (and B) are nearly temperature-independent in the vicinity of transformation temperature. Compared with the elastic data of $\text{Ti}_{50}\text{Ni}_{50}$, $\text{Ti}_{50}\text{Ni}_{30}\text{Cu}_{20}$ shows a similar c_{44} but a 30% lower c' , leading to a 40% higher anisotropy in the vicinity of transformation temperature M_s . More importantly, with approaching transformation temperature, $\text{Ti}_{50}\text{Ni}_{30}\text{Cu}_{20}$ exhibits an increasing anisotropy, while $\text{Ti}_{50}\text{Ni}_{50}$ shows a decreasing anisotropy. These results give some important insight into a long-standing unknown problem why TiNi binary alloy adopts a strange martensite $\text{B19}'$ which is created by a monoclinic $\{001\}\langle 110 \rangle_{\text{B2}}$ shear to the common orthorhombic B19 martensite.

ACKNOWLEDGMENTS

We are grateful to Professor M. Koiwa for allowing us to use the high temperature RPR equipment of his laboratory. This work was supported by a Grant-in-Aid for Research on Priority Area of Phase Transformations and a Grant-in-Aid for International Scientific Research (1997-1999) from the Ministry of Education, Science and Culture of Japan, and partly supported by Project Research A and Shourei (X. R.) from University of Tsukuba.

REFERENCES

- BARSCHE, G. R., and KRUMHANSL, J. A., 1984, *Phys. Rev. Lett.*, **53**, 1069.
 BRILL, T. M., MITTELBAUGH, S. M., ASSMUS, W., MÜLLNER M., and LÜTHI, B., 1991, *J. Phys.: condens. Matter*, **3**, 9621.
 CHUMLYAKOV, YU. I., KIREEVA, I. V., ZUEV, YU. I., and LYISYUK, A. G., 1997, *Mater. Res. Soc. Symp. Proc.*, **459**, 401.
 DEMAREST JR, H. H., 1971, *J. Acoust. Soc. Am.*, **49**, 769.
 GRAY, D. E. (ed.), 1972, *American Institute of Physics Handbook*, 3rd Edn (New York: McGraw-Hill), pp. 2-51.
 HARA, T., OHBA, T., OKUNISHI, E., and OTSUKA, K., 1997, *Mater. Trans. JIM*, **38**, 11.
 HEHEMAN, R. F., and SANDROCK, G. D., 1971, *Scripta metall.*, **5**, 801.
 INOHARA, M., and SUZUKI, T., 1993, *Jpn. J. appl. Phys.*, **32**, 2238.
 KHACHIN, V. N., MUSLOV, S. A., PUSHIN, V. G., and CHUMLYAKOV, YU. I., 1987, *Sov. Phys. Dokl.*, **32**, 606.
 KRUMHANSL, J. A., and GOODING, R. J., 1989, *Phys. Rev.*, **B**, **39**, 3047.
 KUDOH, Y., TOKONAMI, M., MIYAZAKI, S., and OTSUKA, K., 1985, *Acta metall.*, **33**, 2049.
 MAÑOSA, LL., ZARESTKY, J., LOGRASSO, T., DELANEY, D. W., and STASSIS, C., 1993, *Phys. Rev. B*, **48**, 15708.
 MERCIER, O., MELTON, K. N., GREMAUD, G., and HAGI, J., 1980, *J. appl. Phys.*, **51**, 1833.
 MIGLIORI, A., SARAO, J. L., VISSCHER, W. M., BELL, T. M., LEI, M., FISK, Z., and LEISURE, R. G., 1993, *Physica B*, **183**, 1.

- MIURA, N., 1998, MS thesis in progress, University of Tsukuba, Japan.
- NAM, T. H., SABURI, T., KAWAMURA, Y., and SHIMUZU, K., 1990a, *Mater. Trans. JIM*, **31**, 262.
- NAM, T. H., SABURI, T., and SHIMUZU, K., 1990b, *Mater. Trans. JIM*, **31**, 959.
- NISHIYAMA, Z., 1978, *Martensitic Transformation* (New York: Academic Press), pp. 74.
- OHBA, T., RAYMOND, S., SHAPIRO, S. M., and OTSUKA, K., 1998, *Jpn. J. appl. Phys.*, **37**, L64.
- OHBA, T., SHAPIRO, S. M., AOKI, S., and OTSUKA, K., 1994, *Jpn. J. appl. Phys.*, **33**, L1631.
- OHNO, I., 1976, *J. Phys. Earth*, **24**, 355.
- OTSUKA, K., and SHIMIZU, K., 1986, *Int. Met. Rev.*, **31**, 93.
- RAO, C. N. R., and RAO, K. J., 1978, *Phase Transitions in Solids* (New York: McGraw-Hill).
- REN, X., and OTSUKA, K., 1998, *Scripta mater.* (in the press).
- SAKAMOTO, H., TSUZUKI, H., and SHIMIZU, K., 1990, *Mater. Sci. Forum*, **56-58**, 305.
- SHAPIRO, S. M., YANG, B. X., SHIRANE, G., NODA Y., and TANNER, L. E., 1989, *Phys. Rev. Lett.*, **62**, 1298.
- TANAKA, K., ICHITSUBO, T., INUI, H., YAMAGUCHI, M., and KOIWA, M., 1996a, *Phil. Mag. Lett.*, **73**, 71.
- TANAKA, K., OKAMOTO, K., INUI, H., MINONISHI, Y., YAMAGUCHI, M., and KOIWA, M., 1996b, *Phil. Mag. A*, **73**, 1475.
- TANIWAKI, K., 1998, MS thesis, University of Tsukuba, Japan.
- VERLINDEN, B., and DELAHEY, L., 1986, *Proceedings of the International Conference on Martensitic Transformations* (Sendai: The Japan Institute of Metals), p. 768.
- ZIRINSKI, S., 1956, *Acta metall.*, **4**, 164. (Zirinski gave only the elastic compliance data. The corresponding elastic stiffness data was calculated by NAKANISHI, N., 1980, *Prog. mater. Sci.*, **24**, 143).